View metadata, citation and similar papers at core.ac.uk
brought to you by CORE
provided by Publications of the IAS Fellows

High-frequency vertical profiling of meteorological parameters using AMF1 facility during RAWEX–GVAX at ARIES, Nainital

Manish Naja[1,*], Piyush Bhardwaj[1], Narendra Singh[1], Phani Kumar[1], Rajesh Kumar[2], N. Ojha[1], Ram Sagar[3], S. K. Satheesh[4,5], K. Krishna Moorthy[6] and V. R. Kotamarthi[7]

[1]Aryabhatta Research Institute of Observational Sciences, Nainital 263 002, India
[2]National Center for Atmospheric Research, Boulder, Colorado, USA
[3]Indian Institute of Astrophysics, Bengaluru 560 034, India
[4]Centre for Atmospheric and Oceanic Sciences, Indian Institute of Science, Bengaluru 560 012, India
[5]Divecha Centre for Climate Change, Indian Institute of Science, Bengaluru 560 012, India
[6]Indian Space Research Organization, Head Quarters, Bengaluru 560 231, India
[7]Argonne National Laboratory, Argonne, IL, USA

An extensive field study, RAWEX–GVAX, was carried out during a 10-month (June 2011–March 2012) campaign at ARIES, Nainital and observations on a wide range of parameters like physical and optical properties of aerosols, meteorological parameters and boundary layer evolution were made. This work presents results obtained from high-frequency (four launches per day), balloon-borne observations of meteorological parameters (pressure, temperature, relative humidity, wind speed and wind direction). These observations show wind speed as high as 84 m/s near the subtropical jet. It is shown that reanalysis wind speeds are in better agreement at 250 hPa (altitude of subtropical jet) than those above or below this value (100 hPa or 500 hPa). These observations also demonstrate that AIRS-derived temperature profiles are negatively biased in the lower altitude region, whereas they are positively biased near the tropopause. WRF simulated results are able to capture variations in temperature, humidity and wind speed profile reasonable well. WRF and AIRS-derived tropopause height, tropopause pressure and tropopause temperature also show agreement with radiosonde estimates.

Keywords: Aerosols, radiosonde, subtropical jet, tropopause folding, vertical profiling.

Introduction

DYNAMICAL, physical and chemical processes controlling different meteorological systems, including monsoon systems, are poorly understood over South Asia[1,2], where anthropogenic emissions of aerosols and trace gases have been increasing rapidly due to fast economic growth. Higher water vapour and intense solar radiation make this region further complex for understanding the different regional issues related to climate change. The monsoon system over Asia is one of the largest regional climate phenomena and has major influence on the regional atmospheric composition. The Asian monsoon circulation provides an effective pathway for pollution from South Asia to enter the tropical tropopause layer[3] and the stratosphere[4], and thereby influence radiation budget, chemical composition and air quality over a wide region.

Coupling between the stratosphere and troposphere by way of chemical, radiative and dynamical processes plays an important role in climate change. This becomes more critical in tropical regions where the tropopause shows several structures[5]. It has also been shown that stratosphere-to-troposphere transport is pronounced and persistent along the subtropical jet stream[6]. However, meteorology and dynamical aspects, including the transport pathways in this region remain poorly understood and quantified. Despite this, the Asian tropical troposphere is least studied and observations are rather sparse.

During the Indian Ocean Experiment (INDOEX) field studies, aerosols from the Ganges Valley region were shown to affect cloud formation and monsoon activity over the Indian Ocean. Additionally, satellite-based measurements and those from a network of observatories established under ISRO–GBP have shown that the Indo-Gangetic Plain has some of the highest observed aerosol optical depths, broadly indicating lower incoming solar radiation. This region is situated just south of the pristine Himalayan region. Inter Tropical Convergence Zone (ITCZ) also reaches this region, adding more complexity. Further, the chemical characteristics of the South Asian emissions are different from those in other parts of the world because of their disproportionately large contribution from biofuel and biomass burning, making this region a unique place for tropospheric studies.

*For correspondence. (e-mail: manish@aries.res.in)

Considering the importance of this region, a complex field study, Regional Aerosols Warming Experiment–Ganges Valley Aerosol Experiment (RAWEX–GVAX), was planned jointly with Department of Energy (USA), IISc (India), DST (India) and ISRO (India), and observations of a wide range of parameters like physical and optical properties of aerosols, meteorological parameters and boundary layer evolution were made using the first ARM (atmospheric radiation measurement) Mobile Facility (AMF-1) for a 10-month campaign at ARIES, Nainital (29.4°N, 79.5°E; 1950 m amsl). Scientific objectives of the campaign and studies on the properties of aerosols are presented in other articles in this issue. This work focuses on the results obtained from high-frequency balloon-borne observations of meteorological parameters during the campaign.

Balloon-borne meteorological observations are being made by India Meteorological Department (IMD) from different stations in the country, typically twice a day. However, there is no observation in the Himalayan region. Thus, balloon-borne observations of meteorological parameters with four launches in a day, were made in the region continuously for about ten months during 2011–12. Observed seasonal variations in the meteorological profiles are discussed, and possible biases in space-borne sensors and reanalysis products are described. It is shown that temperature profiles from Atmospheric Infrared Sounder (AIRS) have negative bias in the lower altitude region, and positive bias near the tropopause. Variations in tropopause temperature, pressure and its heights are discussed along with the subtropical jet stream over India.

Observation site and set-up

Balloon-borne radiosonde observations were carried out at ARIES. Sharply peaking mountains are located to the north and east of Nainital. There is no industry in Nainital and the total population of Nainital district is about 1 million, out of which about 0.4 million is in Nainital city. The nearby cities of Haldwani and Rudrapur are 20–40 km away from Nainital towards the southern plains, and have small-scale industries. The wind pattern is generally westerly or northwesterly during winter that changes to southwesterly during summer monsoon, while the air masses circulate over the northern Indian region during spring and autumn[7,8].

Experimental set-up: balloon-borne sounding system

During the RAWEX–GVAX campaign, the meteorological balloons with radiosondes were launched four times (0000, 0600, 1200 and 1800 GMT or 0530, 1130, 1730 and 2330 IST) every day; a total of 1069 flights were conducted during June 2011–March 2012 period. These times represent the local conditions of early morning, daytime, evening and midnight. Additionally, radiosonde were also launched at various global sites. In this study we have used data from 1061 successful ascents, while eight flights were discarded as they did not go beyond 5 km altitude. A few test flights were carried out during May 2011 and fully operational flights were commenced from 1 June 2011 (Table 1). The balloon-borne sounding system (BBSS) of AMF-1 is a Vaisala DigiCORA III that comprises of Vaisala RS92-SGP radiosonde, Vaisala GC25 ground check set, GPS omnidirectional antenna and UHF antenna. The RS92-SGP radiosonde has sensors for measurements of pressure, temperature and relative humidity. The humidity sensor (H-HUMICAP) is a thin film capacitor, and the capacitance between its electrodes (dielectric medium) is sensitive to the amount of water vapour present in atmosphere. The temperature sensor (F-THERMOCAP) consists of two platinum wires separated by a glass–ceramic dielectric, whose permittivity is a strong function of temperature. The pressure sensor (BAROCAP) is a micromechanical sensor that is based on changes in the dimensions of the silicon membrane. When pressure is applied, the silicon membrane bends and the vacuum gap between electrodes changes, thus changing capacitance. The PTU sensors are highly sensitive with a response time of <1 sec. Table 2 shows the precision and accuracy of these sensors.

Radiosonde also includes a GPS unit which is used to calculate wind speed and wind direction during flight. Rubber balloon (350 g) from Totex is filled with helium gas for ~15 min at 15 psi pressure in a specially designed hub. The ascent rate of the balloons is about 5 m s^{-1} and

Table 1. Successful balloon flights from 1 June 2011 to 31 March 2012

Month/ flight time (h)	0530	1130	1730	2330	Daily total
June	3	6	3	0	12
July	31	29	30	28	118
August	29	30	27	26	112
September	28	30	30	30	118
October	25	30	31	31	117
November	26	30	29	29	114
December	29	30	31	30	120
January	30	30	31	31	122
February	26	27	29	30	112
March	30	30	28	28	116
	257	272	269	263	1061

A total of 1069 flights were carried out. Eight of them did not cross an altitude beyond 5 km and were discarded from further analysis; thus using 1061 flights during the 10-month period.

Table 2. Precision and accuracy of radiosonde in different height ranges

Measurement error (mbar)	775–200	200–100	100–10
Precision (%)	±4 to ±12	±3 to ±12	±3
Accuracy (%)	±1 to ±12	±1 to ±12	±1 to ±4

generally balloon burst altitude is around 20–25 km. Duration of complete flight (ascent only) is 1–1.5 h. As mentioned earlier, balloons with radiosonde were launched four times in a day (Figure 1). Variability in the launch time was mainly due to constraints of flight permissions from the Air Traffic/Navigation Controllers of this region (Pantnagar and Bareilly).

Results

Figure 1 *b* shows the latitude–longitude distribution of all 1061 balloons flown from ARIES. It can be seen that majority of the balloons drifted to the east (into a northeast–southeast cone). This pattern dominated at higher altitudes and during winter/spring.

Variations in meteorological parameters

Figure 2 shows the variations in observed pressure, temperature, relative humidity and wind speed at 1130 IST from June 2011 to March 2012 up to 20 km altitude. As expected, pressure decreases exponentially with increasing altitude. Near-surface temperature is highest during summer monsoon (~15°C) and lowest during winter (~6°C). The variability in near-surface temperature is lower during summer monsoon than in other seasons. Temperature in the lower–middle troposphere shows seasonal variation somewhat similar to that near the surface. However, the variations are different in the upper troposphere, where the maximum temperature is seen during winter. Temperature also shows greater variability near the tropopause (~18 km) region in winter. Relative humidity (RH) profiles show large variabilities over this region (Figure 2 *c*). While near-surface RH values are highest during summer monsoon, dominance of dry air is seen during winter. Prevalence of cloudy–rainy conditions leads to RH maximum during summer monsoon.

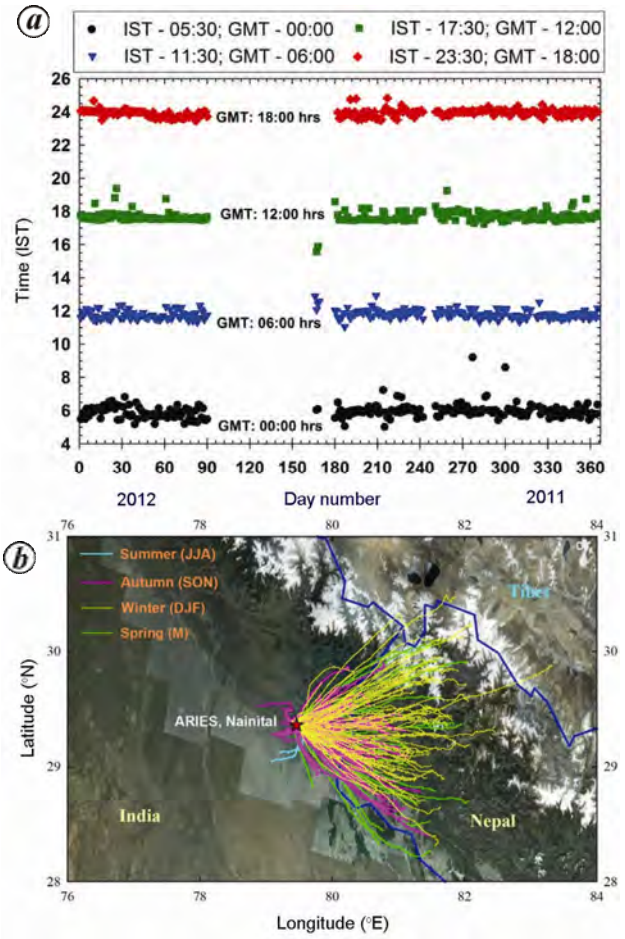

Figure 1. ***a***, Variations in balloon launch time, four times in a day, during June 2011–March 2012. ***b***, Location of the observation site (ARIES, Nainital, 29.4°N, 79.5°E, 1958 m amsl) and path of all the balloons flown during RAWEX–GVAX field campaign.

Wind speed shows a prominent vertical profile with strongest winds in the middle troposphere in all the seasons except summer monsoon. Wind data could not be collected during June–August due to some technical problem. Near-surface wind speed is stronger during spring/autumn and weaker during winter, whereas in the lower to upper tropospheric altitudes, wind speeds are strongest during winter and weakest during summer monsoon. The seasonally averaged peak wind speeds are strongest (~70 m s^{-1} at 11.5 km) during winter and moderately high during spring (~40 m s^{-1} at 12 km) and autumn (36 m s^{-1} at 12.1 km). During summer monsoon, wind speed does not show a clear maximum in the profile and winds are moderately stronger in the middle–upper troposphere (~14 m s^{-1}).

The presence of very strong winds (40–80 m s^{-1}) in the middle–upper troposphere, observed more frequently during winter and occasionally during spring and autumn, is suggested to be associated with the prevailing subtropical jets. The stronger winds could bring pollution from upwind to above the Himalaya, while emissions uplifted from this region, could be transported downwind on faster timescales. This also indicates stronger dynamical processes in the middle–upper troposphere, particularly during winter, which is consistent with the suggested possibility of the wintertime multiple tropopause. Additionally, RH values are much lower in the middle–upper troposphere during winter. These aspects will be discussed in more detail later.

Figure 3 shows the monthly variations in wind direction at different altitudes over central Himalaya in the form of percentage occurrences in four wind direction bands of 90°. The dominance of westerly winds is clearly visible (62–77% in the 2–4 km range) during winter and spring in the lower troposphere. Maximum contribution during summer monsoon is from the easterly winds (42%) in the 2–4 km range[9]. The westerly winds also contribute significantly during summer monsoon in the 4–6 km range (~36%). Variations in the wind direction are different at higher altitudes (8–12 km), where contributions from all the directions other than westerly are less (0–8%) during all seasons, except summer monsoon.

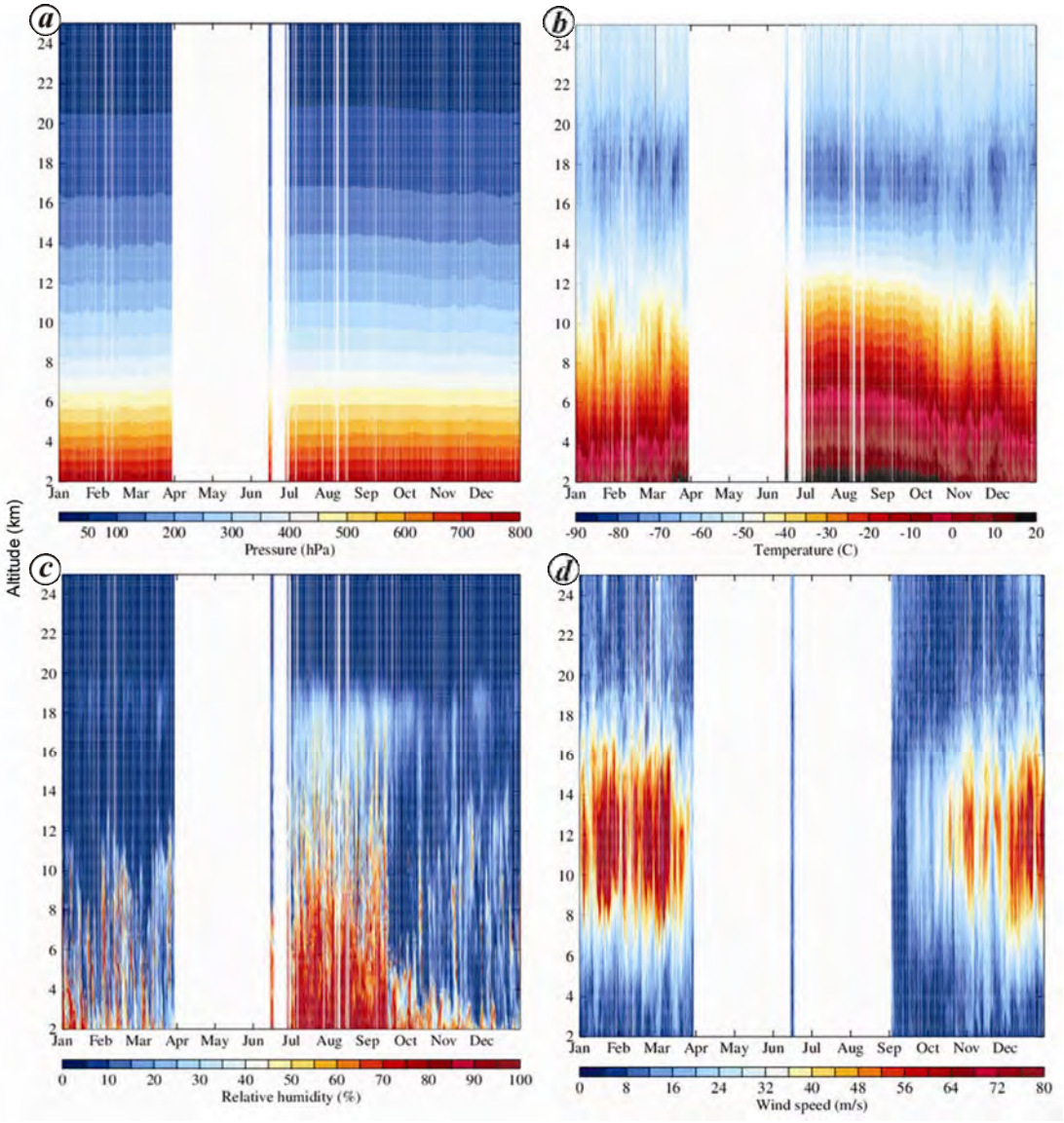

Figure 2. Contour maps showing altitude variations in daily balloon-borne observations of (***a***) pressure, (***b***) temperature, (***c***) relative humidity, (***d***) wind speed during June 2011–March 2012 at 1130 IST in ARIES, Nainital.

Comparison with i-Met radiosonde

Apart from radiosonde from Vaisala (RS92-SGP), radiosonde is from i-Met (iMet-1-RSB 403 MHZ GPS)[9] were also flown together during five occasions (7 February, 29 February, 7 March, 14 March and 29 March) in 2012 to compare both types of sensors. Data from both the sensor were averaged in the bin of 100 m resolution. The average temperature, relative humidity and wind speed profiles show good agreement with square of correlation coefficient of 0.95–0.99 (Figure 4). During all five days, temperature profiles show r^2 of 0.99 and average iMet temperature is higher by 0.3°C. RH and wind speed also show good correlations, 0.95–0.99 and 0.98–0.99 respectively. These parameters are observed to be slightly higher with iMet (RH by 4.9 and wind speed by 0.21).

Simulations with WRF model

Observed temperature, RH and wind speed profiles were also compared with weather research and forecasting (WRF)-simulated profiles during summer monsoon (July 2011) and winter (January 2012; Figure 5). Wind observations were not available in July and are shown for September. In this study WRF model version 3.4.1 is used. The model set-up consists of two nested domains (45 and 15 km) and it is defined on a Mercator projection. The parent domain at 45 km horizontal resolution is defined from 10–40°N, 66–100°E in north–south and east–west directions respectively, and nested domain at 15 km resolution over the 21–34°N, 70–90°E region. The model consists of 51 vertical levels from the surface to 10 hPa (~30 km) and simulations were done for a period of 10 months from

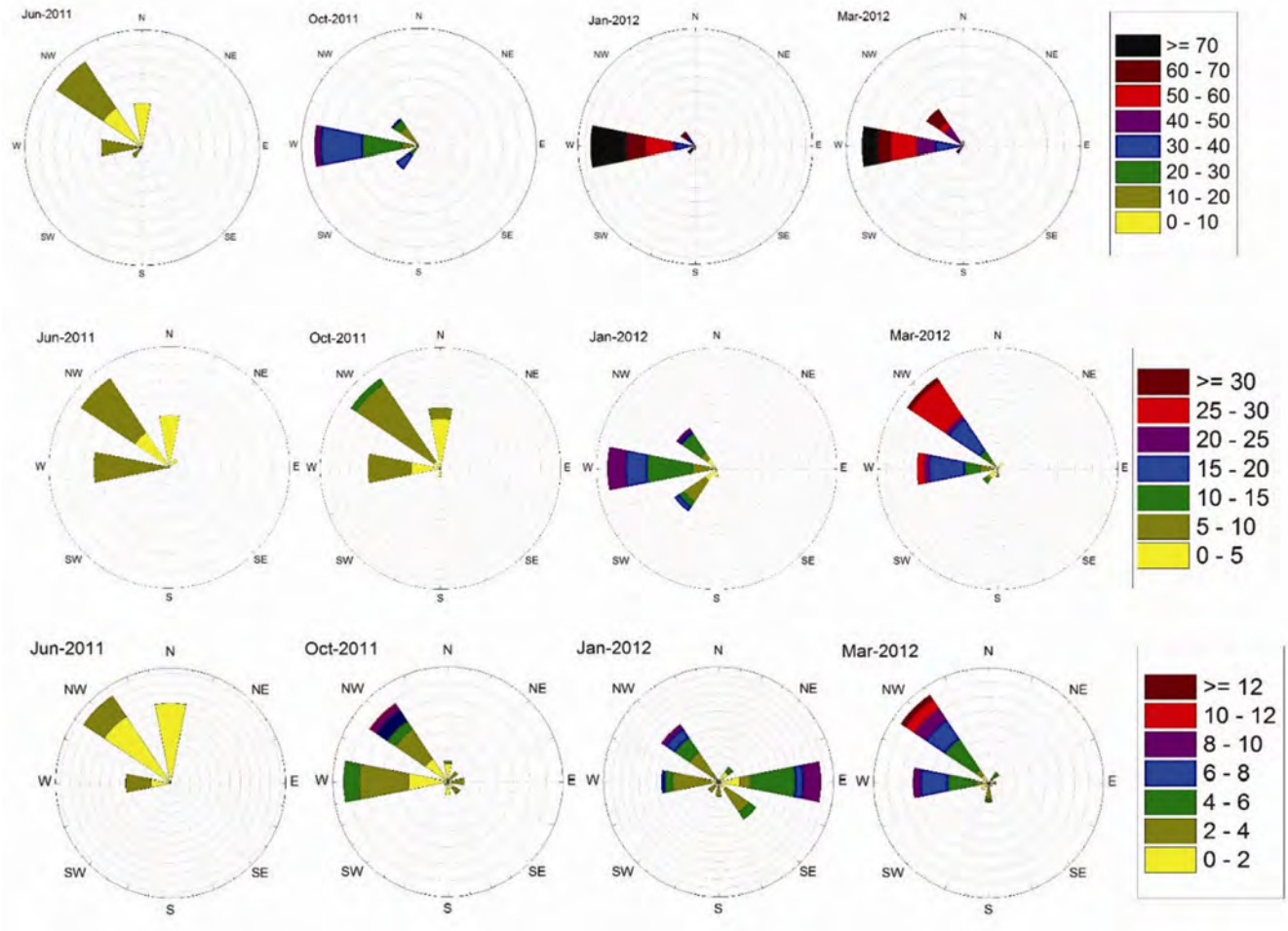

Figure 3. Wind rose plots at 2, 5 and 10 km (bottom to top) altitude during June 2011, October 2011, January 2012 and March 2012 at ARIES, Nainital.

June 2011 to March 2012. The different physics options were adapted from earlier work[10,11]. The static geographical data from United States Geological Survey (USGS) were processed using WRF preprocessing system (WPS). The boundary conditions for the meteorological fields were obtained from National Center for Environmental Predictions (NCEP) Final Analysis (FNL) data at 6 h temporal resolution and 1° × 1° spatial resolution.

Model-simulated temperature, RH and wind speed profiles are in reasonably good agreement with the observations. Temperature profiles show almost no difference to ± 2.2°C in January 2012 and –2.1°C to 6.5°C in July 2011 in different altitude regions (Table 3). Compared to these, RH shows more differences, particularly in the lower troposphere and middle-to-upper troposphere. Observation and model-simulated values both agree reasonably well and show strong winds around 9–13 km with very high values in winter. This confirms the presence of subtropical jet stream in this region and period. Model-simulated wind speed is lower by about 5 m/s in the 9–13 km region during winter compared with the observations.

Seasonal variations in wind speed near subtropical jet

Seasonal variations in wind speed from radiosonde data were further studied in the region of subtropical jet, i.e. 250 hPa and compared with 100 and 500 hPa regions (Figure 6). Maximum speed is observed during winter (57.9 ± 13.6 m s^{-1}) and minimum during summer monsoon (12.7 ± 7.5 m s^{-1}). Variability in wind speed is seen to be greater during January, with speed as high as about 84 m s^{-1} and lowest is about 2 m s^{-1} during September. Wind speed follows nearly similar monthly variations at the higher (100 hPa) and lower altitude (500 hPa) regions. Figure 6 also shows seasonal variations in wind speed derived from Modern Era Retrospective-Analysis for Research and Application (MERRA). These are found to be in reasonable agreement with the observed winds at all three altitudes. Wintertime average MERRA winds (54.3 ± 13.4 m s^{-1}) are more or less similar to those observed from radiosonde at 250 hPa (Table 4). Such similarity is also seen between MERRA (35.2 ± 7.0 m s^{-1}) and radiosonde winds (35.1 ± 9.7 m s^{-1}) at 100 hPa and

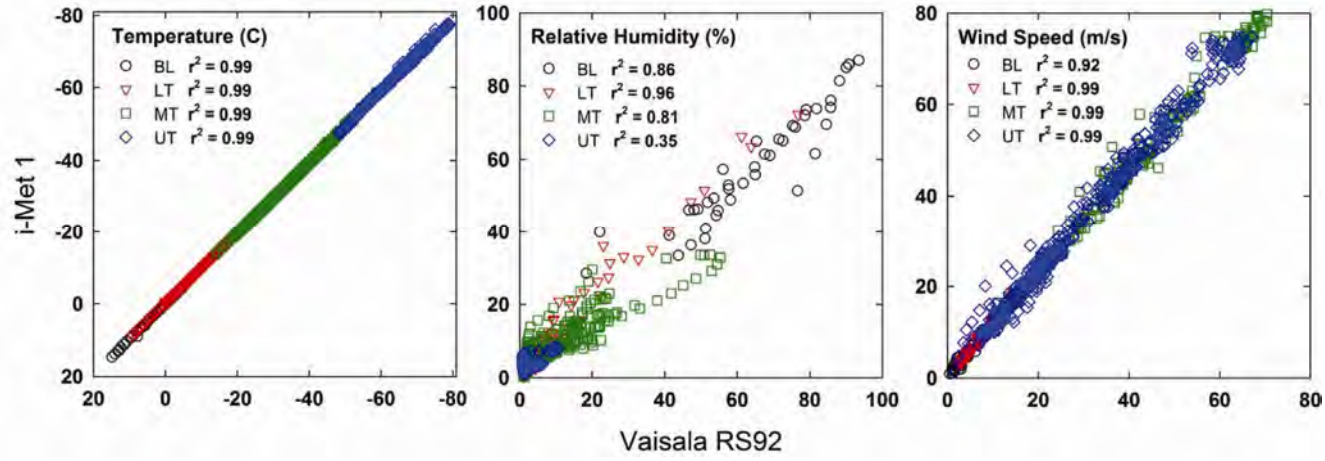

Figure 4. Comparison between Vaisala and i-Met observations of temperature, relative humidity and wind speed during five inter-comparison flights on 7 February, 29 February, 7 March, 14 March and 29 March 2015. Data are classified in the BL (boundary layer) (up to 3 km), LT (lower troposphere) (3–6 km), MT (middle troposphere) (6–12 km) and UT (upper troposphere) (12–18 km) regions.

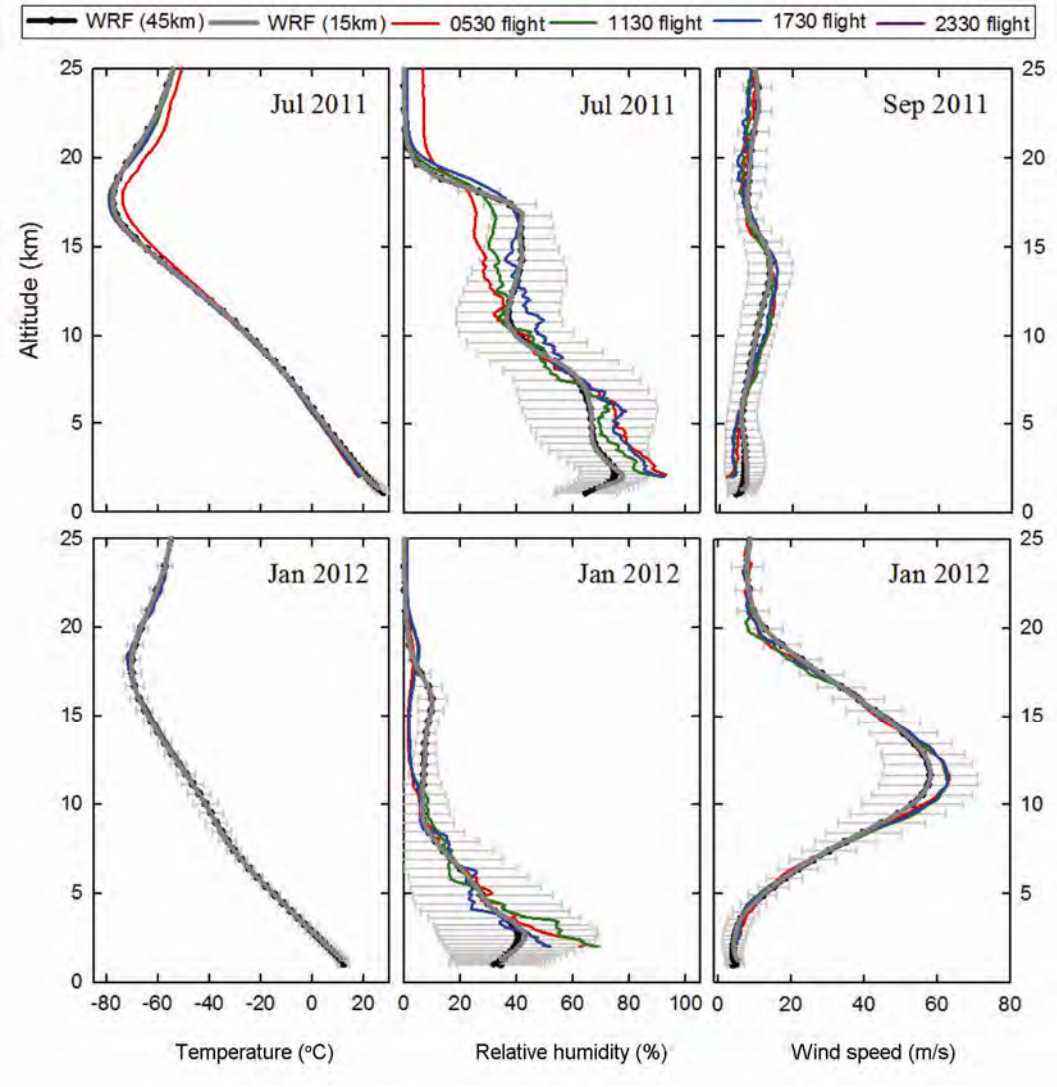

Figure 5. Vertical distribution of temperature, relative humidity and wind speed from radiosonde observations and WRF model simulations during winter (January 2012) and summer monsoon (July 2011). Wind speed is not available for July and is shown for September 2011.

Table 3. Differences (radiosonde – model) between observed temperature, relative humidity (RH), and wind speed and model-simulated data for five altitude regions

	Difference in temperature (%)		Difference in RH (%)		Difference in wind speed (%)	
Altitude region (km)	January 2012	July 2011	January 2012	July 2011	January 2012	September 2011
2–05	–2.2 (40)	–2.8 (–25)	3.8 (9)	9.3 (12)	0.9 (14)	–2.9 (–69)
5–10	–0.5 (1.7)	0.2 (–2)	0.3 (2)	3.4 (6)	1.4 (4)	0.6 (7)
10–15	0.8 (–1)	1.8 (–4)	–4.4 (–139)	–2.5 (–7)	3.1 (5)	1.5 (11)
15–20	–0.8 (1)	1.6 (–2)	–3.4 (–104)	–2.4 (–9)	–4.8 (–19)	–1.0 (–13)
20–25	2.2 (–4)	2.5 (–4)	0.9 (62)	3.1 (85)	–1.1 (–13)	–1.9 (–24)

Negative values indicate that model values are higher than the observed values and vice-versa. Percentage differences are shown in brackets.

Table 4. Average wind speed from radiosonde and Modern Era Retrospective-Analysis for Research and Applications at the three pressure levels

	DJF		JJAS	
Pressure level (hPa)	MERRA	Radiosonde	MERRA	Radiosonde
100	35.2 ± 7.0	35.1 ± 9.7	9.0 ± 4.1	8.5 ± 3.7
250	54.3 ± 13.4	57.9 ± 13.6	10.3 ± 7.1	12.7 ± 7.5
500	18.9 ± 5.7	19.4 ± 6.8	4.5 ± 2.6	5.1 ± 2.8

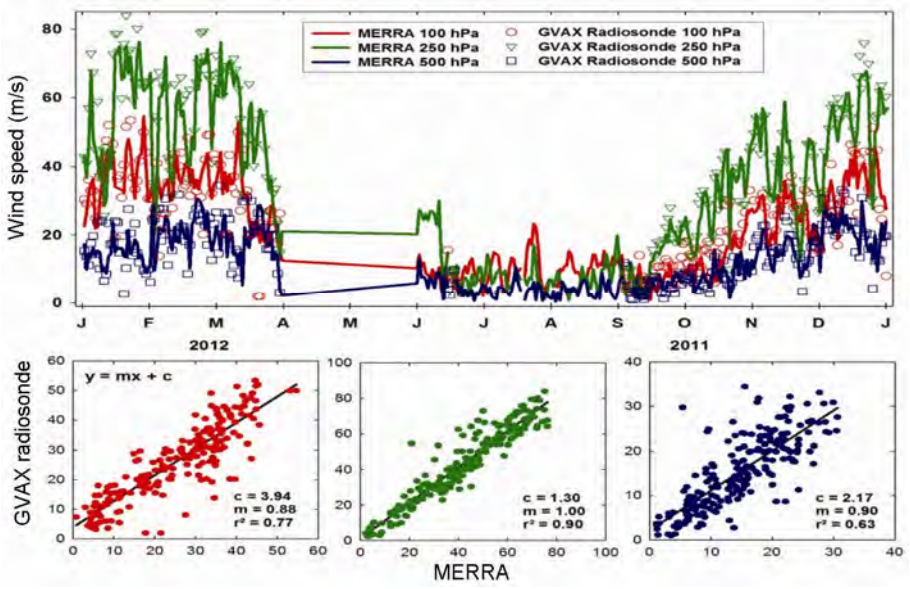

Figure 6. Monthly variations in observed and MERRA wind speed at peak altitude of subtropical jet, i.e. 250 hPa, and also at 100 and 500 hPa. Correlation between them in the three altitude regions is also shown.

500 hPa (18.9 ± 5.7 m s^{-1} and 19.4 ± 6.8 m s^{-1}). Correlation between MERRA and radiosonde winds is positive (r^2 = 0.9) at 250 hPa. The correlation is slightly lower at 100 (0.77) and 500 hPa (0.63).

Biases in temperature profile of AIRS

Temperature profiles from AIRS are found to be more or less in agreement, in terms of altitude variation, with the average temperature profiles of radiosonde (Figure 7). Correlation between radiosonde and AIRS temperatures is positive (r^2 ~ 0.9). However, AIRS data show a negative bias (AIRS temperature lower than radiosonde temperature) of about 5°C in the lower tropospheric region. This bias is mainly from the lower altitude region (Figure 8), except in summer, when this bias is seen at higher altitude also. Both datasets show the lowest temperature in winter and highest temperature during summer monsoon in the lower troposphere.

Figure 8 also provides detailed information of the temperature variations from radiosonde and AIRS data in the tropopause region. In general, monthly variations in both the datasets are similar; however month-to-month variations are greater in case of radiosonde data. It is to be noted that the AIRS temperature shows positive bias in the tropopause, in contrast to the lower troposphere region where AIRS temperature show negative bias (Figure 8). Additionally, tropopause altitude is somewhat higher in the case of radiosonde. This will be discussed further in the next section.

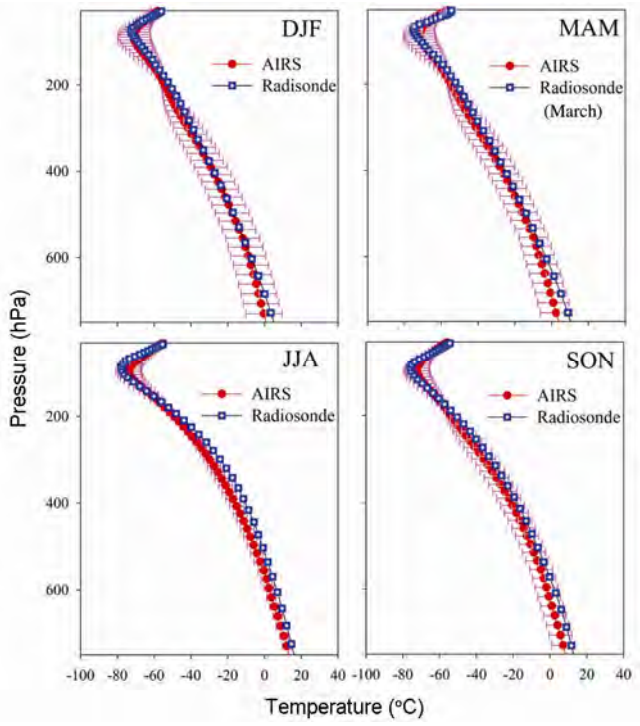

Figure 7. Seasonal average temperature profiles from radiosonde and AIRS. Radiosonde observations are available only during March in spring.

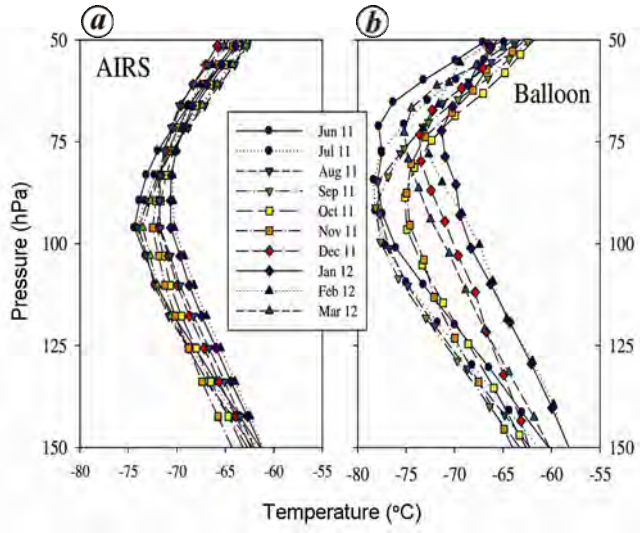

Figure 8. Radiosonde monthly average temperature (°C) profile and data retrieved from AIRS over the central Himalaya in the (***a***) lower troposphere (600–800 hPa) and (***b***) upper troposphere–lower stratosphere region (150–50 hPa) from June 2011 to March 2012.

Seasonal variations in the tropopause

Figure 9 shows seasonal variations in the tropopause pressure, temperature and height, estimated from radiosonde observations (1130 IST). The tropopause height is 16–17 km with pressure of about 100 hPa and temperature of about 200 K. Tropopause pressure is calculated using WMO's criteria. According to this, the lowest level at which the lapse rate decreases to 2 K km^{-1} or less, provided that the average lapse rate between this level and all higher levels within 2 km does not exceed 2 K km^{-1}. We have further discarded profiles having tropopause height less than 12 km, this has led to the removal of 62 profiles. The tropopause height and the temperature are defined corresponding to the determined pressure. These are also estimated from WRF model results and AIRS using the same definition. Tropopause shows greater variability during winter and early spring, while it is almost stable in summer monsoon and early autumn. Greater variations during winter are mainly due

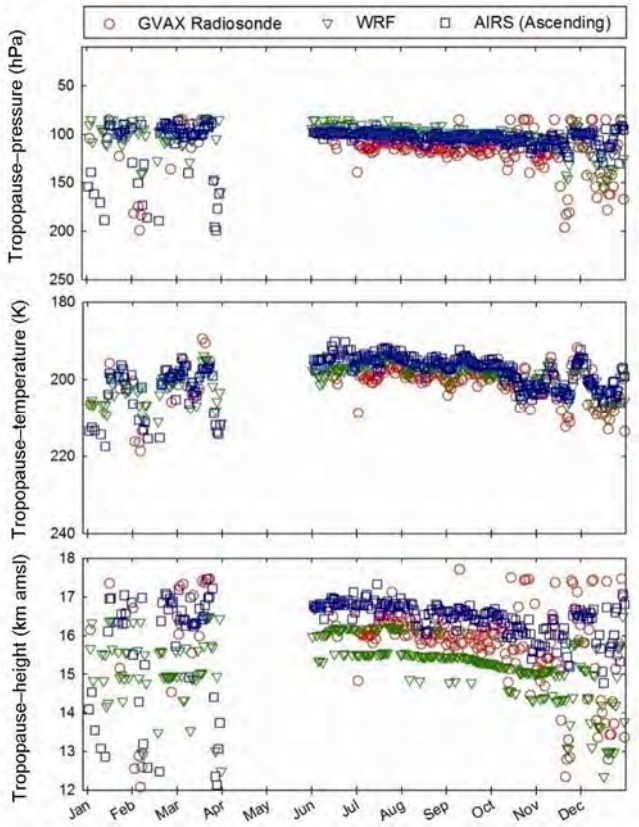

Figure 9. Seasonal variation in the estimated tropopause pressure, temperature and height from radiosonde observations. Estimations from WRF model results and space-borne (AIRS) sensors are also shown.

to double tropopause and tropopause break[10]. The tropopause height is shown to have greater deviation (30–40 hPa) in the subtropics than in the tropics[3] (10–20 hPa).

Discussions and conclusion

The study presents results obtained from high-frequency balloon-borne observations of meteorological parameters. These observations show wind speed as high as 84 m/s near the subtropical jet. It is shown that reanalysis wind speeds are in better agreement at 250 hPa (altitude of subtropical jet) than those at 100 or 500 hPa. The observations also demonstrate that AIRS temperature profiles are negatively biased in the lower altitude region, while they are positively biased near the tropopause. WRF simulated results are able to capture variations in temperature, humidity and wind speed profile reasonable well. WRF and AIRS-derived tropopause height, pressure, temperature also show good agreement with radiosonde estimates.

The high-frequency profiling of meteorological parameters obtained during this campaign, will be useful in further fine-tuning of the models and improving our understanding of the regional climate system. Better understanding of distribution of key species in the climate-sensitive tropopause region is also possible. For example, the uncertainty in the tropospheric ozone budget is largely associated with the limited knowledge of contributions from the stratosphere–troposphere exchange (STE). Such studies are sparse over the Indian region[12,13] and the role of STE is not well understood.

1. Moorthy, K. K., Aerosol optical depths over peninsular India and adjoining oceans during the INDOEX campaigns: spatial, temporal, and spectral characteristics. *J. Geophys. Res*., 2001, **106**(D22), 28539–28554; doi: 10.1029/2001JD900169.
2. Satheesh, S. K., Moorthy, K. K., Babu, S. S., Vinoj, V. and Dutt, C. B. S., Climate implications of large warming by elevated aerosol over India. *Geophys. Res. Lett.*, 2008, **35**, L19809; doi: 10.1029/2008GL034944.
3. Fueglistaler, S., Dessler, A. E., Dunkerton, T. J., Folkins, I., Fu, Q. and Mote, P. W., Tropical tropopause layer. *Rev. Geophys*., 2009, **47**, RG1004; doi: 10.1029/2008RG000267.
4. Randel, W. J. *et al.*, Asian monsoon transport of pollution to the stratosphere. *Science*, 2010, **328**(5978), 611–613; doi: 10.1126/science.1182274.
5. Reichler, T., Dameris, M. and Sausen, R., Determining the tropopause height from gridded data. *Geophys. Res. Lett*., 2003, **30**, doi: 10.1029/2003GL018240.
6. Trickl, T., Bärtsch-Ritter, N., Eisele, H., Furger, M., Mücke, R., Sprenger, M. and Stohl, A., High-ozone layers in the middle and upper troposphere above Central Europe: potential import from the stratosphere along the subtropical jet stream. *Atmos. Chem. Phys*., 2011, **11**, 9343–9366, doi: 10.5194/acp-11-9343-2011.
7. Naja, M, Mallik, C., Sarangi, T., Sheel, V. and Lal, S., SO_2 measurements at a high altitude site in the central Himalayas: role of regional transport. *Atmos. Environ.*, 2014, **99**, 392–402; doi: 10.1016/j.atmosenv.2014.08.031.
8. Sarangi, T. *et al.*, First simultaneous measurements of ozone, CO, and NO_y at a high-altitude regional representative site in the central Himalayas. *J. Geophys. Res. Atmos.*, 2014, **119**, 1592–1611; doi: 10.1002/2013JD020631.
9. Ojha, N. *et al*., On the processes influencing the vertical distribution of ozone over the central Himalayas: analysis of year-long ozonesonde observations. *Atmos. Environ*., 2014, **88**, 201–211; doi: 10.1016/j.atmosenv.2014.01.031.
10. Kumar, R., Naja, M., Pfister, G. G., Barth, M. C. and Brasseur, G. P., Simulations over South Asia using the weather research and forecasting model with chemistry (WRF-Chem): set-up and meteorological evaluation. *Geosci. Model Dev.*, 2012, **5**, 321–343; doi: 10.5194/gmd-5-321-2012.
11. Kumar, R. *et al*., Effects of dust aerosols on tropospheric chemistry during a typical pre-monsoon season dust storm in northern India. *Atmos. Chem. Phys.*, 2014, **14**, 6813–6834; doi: 10.5194/acp-14-6813-2014.
12. Mandal, T. K., Cho, Y. J. N., Peshin, S. K., Srivastava, S. K., Rao, P. B., Jain, A. R. and Mitra, A. P., Stratosphere–troposphere ozone exchange observed with the Indian MST radar and simultaneous balloon borne ozonesonde. *Radio Sci.*, 1998, **33**(4), 861–893.
13. Ganguly, N. D. and Tzanis, C., Study of stratosphere–troposphere exchange events of ozone in India and Greece using ozonesonde ascents. *Meteorol. Appl.*, 2011, **18**, 467–474; doi:10.1002/met.241.

ACKNOWLEDGEMENTS. RAWEX–GVAX field campaign was jointly organized by ISRO, IISc, ARIES and DOE. We are grateful to the air traffic control for help in coordinating the balloon launches, four times in a day. We also thank project trainees for their help with balloon launches, particularly at 2330 and 0530 IST from ARIES. Support from NASI is highly acknowledged by R.S.

doi: 10.18520/cs/v111/i1/132-140